



The Society for engineering
in agricultural, food, and
biological systems

An ASAE Meeting Presentation

Paper Number: 052006

Estimating Water Quality with Airborne and Ground-Based Hyperspectral Sensing

Kenneth A. Sudduth, Agricultural Engineer

USDA-ARS Cropping Systems and Water Quality Research Unit, Columbia, Missouri

Gab-Sue Jang, Postdoctoral Researcher

Biological Engineering Department, University of Missouri, Columbia, Missouri

Robert N. Lerch and E. John Sadler, Soil Scientists

USDA-ARS Cropping Systems and Water Quality Research Unit, Columbia, Missouri

Written for presentation at the
2005 ASAE Annual International Meeting
Sponsored by ASAE
Tampa Convention Center
Tampa, Florida
17 - 20 July 2005

Abstract. *Remotely sensed estimates of water quality parameters would facilitate efforts in spatial and temporal monitoring. In this study we collected hyperspectral water reflectance data with airborne and ground-based sensing systems for multiple arms of Mark Twain Lake, a large man-made reservoir in northeast Missouri. Water samples were also collected and analyzed in the laboratory for chlorophyll, nutrients, and turbidity. Wavelength-selection (i.e., stepwise multiple regression) methods and previously reported indices were used to develop relationships between spectral and water quality data. Within the single measurement date of this study, all measured water quality parameters were strongly related ($R^2 > 0.6$) to reflectance data from the ground system. Relationships between water quality parameters and airborne reflectance data were generally somewhat lower, but still with $R^2 > 0.6$. Previously developed narrow-band reflectance indices also worked well to estimate chlorophyll concentration. Wide-band, multispectral reflectance, simulating Landsat data, was strongly related only to turbidity and those other parameters (e.g., phosphorus) highly correlated to turbidity in this dataset. Thus, hyperspectral sensing, coupled with calibration sampling, can be used to estimate lake water quality differences, and appears to have advantages over multispectral sensing in this application.*

Keywords. *Water quality, Reflectance, Hyperspectral, Remote sensing*

The authors are solely responsible for the content of this technical presentation. The technical presentation does not necessarily reflect the official position of the American Society of Agricultural Engineers (ASAE), and its printing and distribution does not constitute an endorsement of views which may be expressed. Technical presentations are not subject to the formal peer review process by ASAE editorial committees; therefore, they are not to be presented as refereed publications. Citation of this work should state that it is from an ASAE meeting paper. EXAMPLE: Author's Last Name, Initials. 2005. Title of Presentation. ASAE Paper No. 05xxxx. St. Joseph, Mich.: ASAE. For information about securing permission to reprint or reproduce a technical presentation, please contact ASAE at hq@asae.org or 269-429-0300 (2950 Niles Road, St. Joseph, MI 49085-9659 USA).

Introduction

Impairment of the environment by agricultural activities is an ongoing concern of agriculturalists, environmentalists, and the general public. Many conservation practices, including those designed to reduce losses of soil, nutrients, and pesticides from agricultural fields, have a primary goal of reducing this impairment. Because environmental quality is in the public interest, the US Department of Agriculture (USDA) provides financial incentives to producers for implementing such conservation practices on their lands.

Recently, agencies of the USDA initiated a project to quantify the environmental benefits of conservation practices implemented with USDA funding. This Conservation Effects Assessment Project (CEAP) includes a national assessment led by the USDA Natural Resources Conservation Service and a watershed assessment studies component led by the USDA Agricultural Research Service (ARS) (Mausbach and Dedrick, 2004). The watershed component of CEAP will provide an in-depth study of environmental effects and benefits for select watersheds and provide additional research on conservation practices and their expected effects at the watershed scale.

In Missouri, the ARS Cropping Systems and Water Quality Research Unit is conducting CEAP watershed assessment research in the Salt River basin. The Salt River supplies Mark Twain Lake, a manmade flood control and water supply reservoir in northeast Missouri. The Missouri CEAP research includes a monitoring campaign to characterize the hydrologic balance and nutrient/chemical loading to Mark Twain Lake. The core of this monitoring is stream flow monitoring and water sampling at 13 sites within the basin. Because these monitoring sites are a significant distance upstream from the lake to avoid stagnant conditions at high lake stages, we wished to augment this data with a study of water quality variations among the different arms of the lake. Remote sensing was considered as a potential method to estimate such water quality variations.

Remote sensing of water quality

Research has shown that remote sensing can be used to estimate water quality parameters such as suspended sediments, turbidity, and chlorophyll. Compared to traditional sample collection and analysis approaches, potential advantages of remote sensing include an increased spatial and temporal resolution that may be important for assessment and/or management of water quality.

The potential of remote sensing for water quality estimation was first investigated in the early 1970s, with the development of empirical relationships between spectral properties and water quality measurements. As the science of remote sensing has progressed, biophysical models have been developed for some relationships, but empirical models are still used in many situations. Such empirical models often provide good results. However, it is important to recognize that they may only be valid for the specific conditions under which the data were collected, and that they should be applied under different conditions only with caution and appropriate validation (Ritchie et al., 2003).

The use of remote sensing to quantify suspended sediment has been studied extensively. Suspended sediments increase the energy reflected from surface waters in the visible and near-infrared spectrum. The specific amount of increase depends on sediment type, texture, color, water depth, and viewing conditions (Ritchie et al. 2003). Although reflectance increased at all wavelengths, Ritchie et al. (1976) concluded that wavelengths between 700 and 800 nm were most useful for quantifying suspended sediment concentration. For concentrations below 50 mg

L^{-1} , a linear relationship was sufficient; however, from 50 to 150 $mg L^{-1}$, a curvilinear relationship was needed. Similarly, Lodhi et al. (1998) reported that wavelengths between 700 and 900 nm provided the best results, and that second-order regression models were better than linear models. Furthermore, these authors noted, as did Ritchie et al. (2003), that data from the wide spectral bands available with multispectral aerial and satellite sensors were sufficient for accurate estimation of sediment concentration.

Related to suspended sediment concentration is turbidity, a measure of the degree to which light transmitted through the water is scattered by suspended particles. Although turbidity is also influenced by the quantity and type of organic particulates (e.g., algae) in the water, suspended sediments are usually the dominant particulate matter in surface water, and therefore are the main cause of turbidity. The relationship between sediment concentration and turbidity is influenced by the particle size distribution of the sediment, and thus should be determined for specific watersheds and/or distinct dominant soil types (Hayes et al., 2001). Some research has directly related spectral reflectance to turbidity. For example, Han (1996) achieved a correlation of 0.95 between turbidity and the difference in reflectance at 710 and 720 nm for samples obtained from a reservoir. Shafique et al. (2003) also found good results when correlating turbidity to the difference in reflectance between two wavelengths; however, the wavelength pairs selected were different between two different rivers in Ohio.

Several approaches used to estimate chlorophyll with remote sensing were reviewed by Ritchie et al. (2003). Multispectral approaches have not been successful in waters with high suspended sediment concentrations because these broad-wavelength data cannot successfully discriminate chlorophyll where the spectral signal is dominated by sediment. However, research has shown that narrow-band reflectance data at the “red edge” of the visible spectrum can estimate chlorophyll in the presence of high suspended sediment concentrations. In a study using large outdoor water tanks, Han et al. (1994) found that the (NIR/red) reflectance ratio was independent of suspended sediment concentration over a wide range of sediment levels and two sediment types. They considered the ratio superior to the (NIR-red) difference, which was not completely independent of sediment level. Further outdoor tank research by the same group (Rundquist et al., 1996) found that the derivative of the reflectance curve near 690 nm was a better estimator of relatively high chlorophyll concentrations, while the NIR/red (705/670 nm) ratio was better at low concentrations. In a comparison over multiple measurement dates and sampling sites in a turbid reservoir, the derivative approach was better (Han and Rundquist, 1997). This was particularly apparent when data from multiple measurement dates were combined (derivative $r = 0.82$; ratio $r = 0.55$). Shafique et al. (2003) used the 705/675 nm reflectance ratio to quantify chlorophyll *a* and reported similar results ($r = 0.71$ and 0.72) for two Ohio rivers.

Reports describing the use of remote sensing to characterize or quantify nutrient levels in water are more limited than those describing estimation of sediment or chlorophyll. Shafique et al. (2003) correlated total phosphorus in two Ohio rivers to reflectance ratios. Similar to their work with turbidity described above, different wavelengths were selected for the two rivers.

Objectives

The primary objective of this study was to relate hyperspectral remote sensing information to lake water quality parameters. A subobjective was to compare the results obtained from two sources of hyperspectral data; airborne remote sensing and a portable field spectrometer.

Materials and Methods

Study Site and Sampling Locations

Research was conducted at the 7,530-ha Mark Twain Lake in northeast Missouri. Mark Twain Lake serves as the public drinking water supply for approximately 42,000 people, and consistently high spring and summer time atrazine levels have been an on-going concern. More recently, late summer algal blooms have created the need for more extensive water treatment to reduce odor and taste problems in drinking water and may be a reflection of increased nutrient transport within the basin.

The source of water for Mark Twain Lake is the Salt River system (fig. 1), which encompasses an area of 6,520 km² within portions of 12 northeastern Missouri counties. The Salt River basin has a known and well-documented history of herbicide and sediment contamination problems. The claypan soils that predominate within the basin create a natural barrier to percolation, which promotes surface runoff. This results in a high degree of vulnerability to surface transport of sediment, herbicides, and nutrients. Within the basin, land use is predominately agricultural. The primary row crops are soybeans, corn, and sorghum. Forage production is mainly tall fescue. Livestock production is mainly beef cattle, but swine operations are increasing, particularly in the Middle and Elk Fork watersheds (fig. 1).

Seven sampling sites were identified where highway bridges crossed arms of the lake (fig. 2). These seven sites were identified by the highway name or number, plus a cardinal direction designation if necessary. For example, site 24E (fig. 2) was the easternmost location on U.S. Highway 24. At each site, multiple sampling stations were located along the highway bridge to investigate variation in reflectance and water quality properties across the width of the arm. The number of stations at each site varied from 5 to 11 depending on the width of the arm. The total number of sampling stations was 51.



Figure 1. Salt River basin, showing major watersheds supplying Mark Twain Lake.

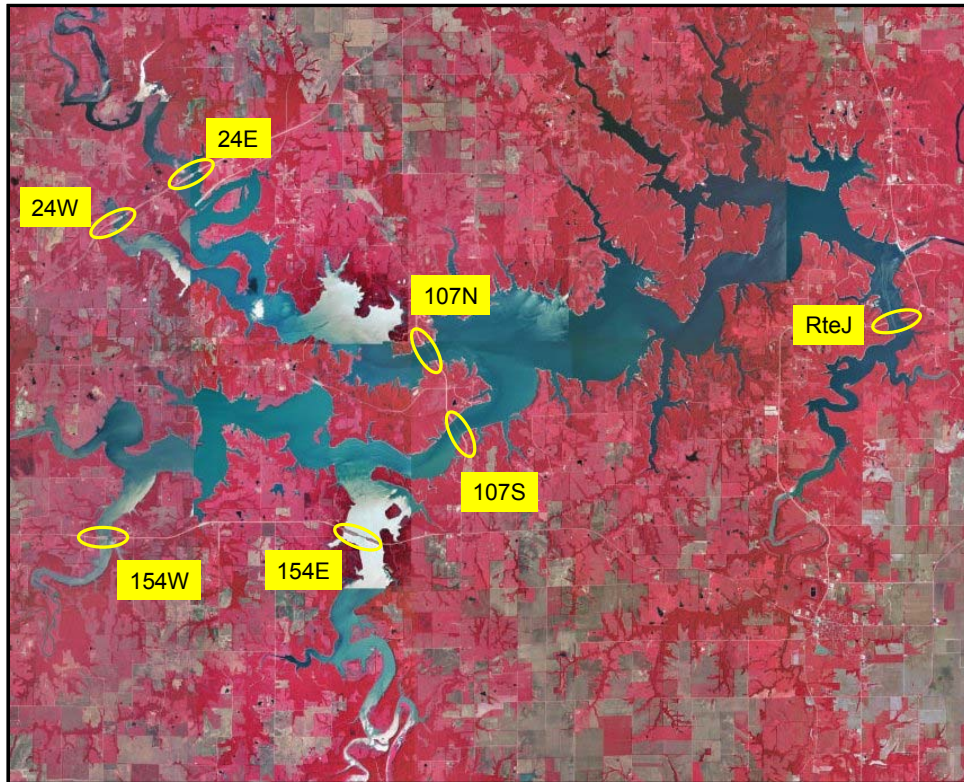


Figure 2. False-color image of Mark Twain Lake, showing seven sampling locations where highway bridges cross arms of the lake.

Data Collection and Processing

Reflectance data and water quality samples were collected on August 30, 2004, between approximately 1045 hr and 1700 hr CDT. Sky conditions at the time of data collection were generally clear with some intermittent cloud cover later in the day. As recorded at Monroe City, Mo., approximately 15 km away, air temperature was 21 to 27° C, and winds were from the west at 1.4 to 1.8 m/s during the sampling period. With these relatively calm winds, the water surface was generally smooth, with little wave action. Monroe City precipitation was 14.5 cm in the 5 days prior to sampling. With this amount of rainfall and the accompanying runoff, lake water levels rose approximately 2 m in the 3 days prior to sampling. We observed that tributaries entering the lake were still flowing briskly at the time of data collection.

Field Spectrometer Data

Data were collected with an ASD FieldSpec Pro¹ FR field spectrometer (Analytical Spectral Devices, Boulder, Colo.) Using a three-detector system, this instrument recorded upwelling radiance from the water surface in the wavelength range of 350 nm to 2500 nm. Optical

¹ Mention of trade names or commercial products in this publication is solely for the purpose of providing specific information and does not imply recommendation or endorsement by the U.S. Department of Agriculture or the University of Missouri.

resolution was 3 to 10 nm, and the sampling interval was 1.4 to 2.0 nm. Light input to the system was through a fiber optic cable with a 1-degree field of view foreoptic attachment.

At each sampling station, the pistol-grip foreoptic was pointed at the water surface 90 degrees from the principal vertical plane of the sun, at a 40-degree angle from nadir. This protocol was suggested to minimize the effects of sun glint on the data collection process (Rick Perk, Center for Advanced Land Management Information Technologies, University of Nebraska, personal communication). In this orientation, the 1-degree foreoptic collected light from an ellipse of approximately 500 cm² on the water surface. Data were collected between 1240 and 1630 hr CST, requiring approximately 15 to 20 minutes at each bridge.

At each sampling station, two radiance data files were stored, with each file containing the mean of 10 individual wavelength scans. Before and after the water data were collected at each bridge, radiance data were collected from a handheld Spectralon reference panel. Data from the Spectralon readings were compared to verify that radiance did not change appreciably during the course of water measurements. In postprocessing, radiance values in each water data file were divided by the preceding reference panel data to obtain apparent reflectance of the water surface as a function of wavelength. The duplicate reflectance datasets at each station were examined for irregularities. Because no obvious outliers were identified, the two duplicate datasets were averaged for analysis.

Because we were primarily interested in using field spectrometer data to supplement aerial image data, we extracted the reflectance data from 350 to 975 nm on a 5-nm interval, resulting in 126 individual points. This was the range sensed by the silicon photodetector in the ASD (higher wavelengths used other detectors), and encompassed all the wavelengths in the aerial images. Two field spectrometer datasets were constructed for analysis – one containing all data and the other containing data at the 26 wavelengths most closely corresponding to the wavelengths of the aerial hyperspectral images.

Aerial Hyperspectral Images

Airborne hyperspectral imaging was completed between 1045 and 1135 hr by personnel from the Center for Advanced Land Management Information Technologies (CALMIT) at the University of Nebraska, using an AISA pushbroom sensor (Specim / Spectral Imaging Ltd., Oulu, Finland) mounted in a single-engine light aircraft. A key feature of the AISA system is that it includes a downwelling irradiance sensor mounted on top of the aircraft, allowing calculation of apparent reflectance at the sensor. Research has verified that the at-sensor reflectance can be used as a surrogate for target reflectance, eliminating the need to deploy calibration standards on the ground (Charles Walthall, USDA-ARS, Beltsville, Md., personal communication).

For this application, the AISA system was configured to provide a 3-m pixel resolution and an approximately 1100-m swath width. Data were collected in 26 user-defined bands within the 400- to 970-nm spectral range of the sensor. Table 1 includes center wavelengths and bandwidths for each channel.

The postprocessing provided by CALMIT radiometrically calibrated and georectified the AISA data. We performed no additional radiometric calibration. However, additional local georectification was completed, using DGPS (approximately 1-m accuracy) points at each end of each bridge where sampling occurred. A separate linear shift was applied to the image data from each bridge to improve alignment of the image coordinates with these DGPS points (fig. 3). Then, data were extracted from the image at each ASD data collection station along each bridge. Two sets of data were extracted, one comprised of a single pixel at each station and the other comprised of a 3x3 pixel grid at each station.

Table 1. Band centers and bandwidths of the AISA system as configured for this study.

Band	Center wavelength, nm	Bandwidth, nm	Band	Center wavelength, nm	Bandwidth, nm
1	498	4	14	649	4
2	528	4	15	658	4
3	539	4	16	673	4
4	548	4	17	682	4
5	558	4	18	689	4
6	569	4	19	699	3
7	583	4	20	704	3
8	590	4	21	709	3
9	598	4	22	714	3
10	609	4	23	719	3
11	623	4	24	745	9
12	631	4	25	810	9
13	638	4	26	844	9



Figure 3. Nine field spectrometer points (dots) overlaid on gray-scale representation of the shifted aerial image for location 107S. DGPS points (stars) at each end of the bridge were used for local georectification of the hyperspectral image.

Water Sampling and Water Quality Analysis

Water sampling was conducted between 1300 and 1700 hr, generally within 30 minutes of the time of field spectrometer data collection. Because one water sample was lost, data were available for only 50 sampling stations. Grab samples were obtained from the top 0.15-0.30 m

of the water column at each sampling station. Each sample, approximately 1 L in volume, was placed on ice while transported to the laboratory and then refrigerated in the laboratory until analyses were performed.

Analyses were conducted for dissolved N and P forms ($\text{NO}_3\text{-N}$, $\text{NH}_4\text{-N}$, and $\text{PO}_4\text{-P}$), total N and P, turbidity, total chlorophyll, chlorophyll a, and pheophytin. For dissolved nutrient analyses, all samples were filtered through 0.45- μm nylon filters within 48-72 hours of collection. Dissolved N and P species were then determined colorimetrically using a Lachat flow injection system (Lachat Instruments, Loveland, Colo.). Total N and P were determined on thoroughly mixed, unfiltered 60-mL samples by autoclave digestion with potassium persulfate (Nydahl, 1978). Persulfate digestion quantitatively converted all N forms to nitrate (NO_3^-) and all P forms to orthophosphate (PO_4^{3-}) which were then determined colorimetrically by the Lachat flow injection system. Turbidity was measured in the laboratory using a YSI 6920 Sonde (YSI, Inc., Yellow Springs, Ohio) with a calibrated turbidity probe. Unfiltered samples were thoroughly mixed, allowed to stand for one minute, and nephelometric turbidity unit (NTU) data were obtained at 6-second intervals for 2 minutes. The average value over the 2 minutes was reported. Total chlorophyll, chlorophyll a, and pheophytin were determined by filtering a known volume of sample through a 0.45- μm filter. The filters were then extracted with 7.6 mL of ethanol in a water bath (21- 23°C) for 15 minutes, allowed to cool for at least 2 hours, and then analyzed using a fluorometer at the appropriate wavelength for each of the three analytes.

Results and Discussion

Water Quality Data

With the exception of total N, each measured water quality parameter varied considerably, with a standard deviation of the same order of magnitude as the mean. Variation within each sampling location was generally much less than the overall variation, with the exception of location 107S (table 2). At that location, a distinct flow path along the south shore was considerably different, both optically (fig. 3) and in terms of water quality parameters, from the rest of the arm.

When considering the overall dataset, significant ($\alpha = 0.05$) correlations were observed between most variable pairs (table 3). Highest correlations ($r > 0.9$) were found among the three chlorophyll measurements and between total P and dissolved $\text{PO}_4\text{-P}$. Relatively high positive correlations ($r > 0.5$) with turbidity were found for $\text{NH}_4\text{-N}$, $\text{PO}_4\text{-P}$, and total P. Relatively high negative correlations ($|r| > 0.5$) were found between $\text{PO}_4\text{-P}$ and the three chlorophyll measurements. This level of correlation suggested that similar relationships with reflectance data might be found for the three chlorophyll measurements and for the two phosphorus measurements.

Field Spectrometer Data

As an initial screening, correlations between optical density (OD) and the water quality parameters were graphed (fig. 3). Optical density, $\log(1/\text{reflectance})$, was used rather than reflectance because, assuming Beer's Law applies, absorbance (or OD) should be linearly related to the concentration of the absorbing substance (e.g., chlorophyll, sediment). Generally, the highest correlations were found at wavelengths above 650 nm. Above 930 nm, the corelograms became unstable, assumedly due to the lower signal-to-noise ratio observed at the highest wavelengths.

Table 2. Means and (in parentheses) standard deviations of water quality measurements, both overall and for each sampling location.

	Overall	24W	24E	107N	107S	154E	154W	RteJ
Total chlorophyll, $\mu\text{g L}^{-1}$	24.1 (21.8)	2.7 (0.56)	5.9 (1.2)	29.6 (9.7)	57.7 (25.9)	25.3 (6.9)	11.4 (3.0)	12.7 (1.6)
Chlorophyll a, $\mu\text{g L}^{-1}$	21.1 (19.7)	2.0 (0.43)	4.7 (1.1)	25.9 (8.7)	51.6 (23.4)	21.5 (6.4)	9.6 (2.9)	11.0 (1.3)
Pheophytin, $\mu\text{g L}^{-1}$	8.0 (5.4)	1.7 (0.34)	3.1 (0.26)	10.0 (3.1)	15.6 (5.6)	10.2 (1.5)	4.8 (0.6)	4.7 (0.8)
Turbidity, NTU	18.3 (22.2)	31.9 (18.8)	25.6 (27.9)	5.0 (2.0)	9.6 (3.5)	21.6 (6.0)	66.1 (11.8)	0.1 (0.2)
Total N, mg L^{-1}	1.15 (0.19)	0.91 (0.03)	1.30 (0.17)	0.98 (0.07)	1.29 (0.20)	1.26 (0.12)	1.32 (0.04)	1.06 (0.06)
Dissolved $\text{NO}_3\text{-N}$, mg L^{-1}	0.25 (0.10)	0.13 (0.08)	0.24 (0.02)	0.17 (0.02)	0.22 (0.06)	0.35 (0.01)	0.24 (0.01)	0.42 (0.05)
Dissolved $\text{NH}_4\text{-N}$, mg L^{-1}	0.015 (0.017)	0.013 (0.010)	0.026 (0.009)	0.005 (0.004)	0.006 (0.005)	0.022 (0.011)	0.045 (0.009)	0.010 (0.028)
Total P, mg L^{-1}	0.16 (0.12)	0.33 (0.01)	0.33 (0.04)	0.05 (0.01)	0.10 (0.02)	0.15 (0.03)	0.32 (0.03)	0.03 (0.01)
Dissolved $\text{PO}_4\text{-P}$, mg L^{-1}	0.059 (0.078)	0.234 (0.006)	0.129 (0.004)	0.002 (0.001)	0.007 (0.002)	0.044 (0.007)	0.133 (0.001)	0.003 (0.004)
# of observations	50	5	6	11	9	6	5	8

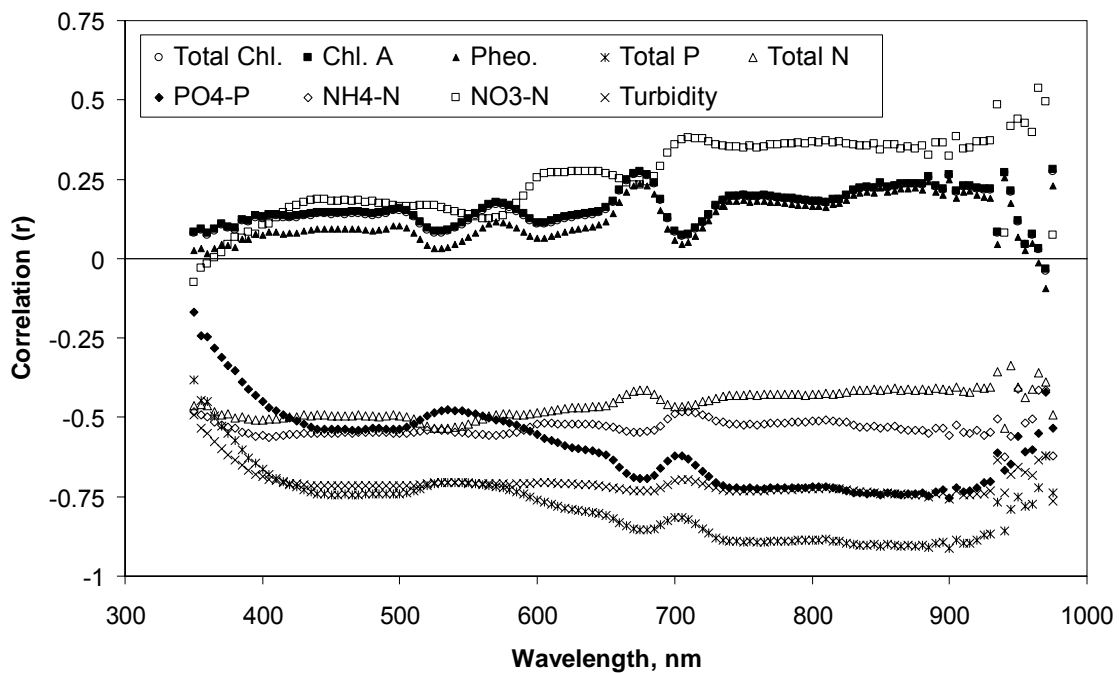


Figure 3. Correlation between water quality parameters and OD-transformed field spectrometer data.

Table 3. Significant ($\alpha= 0.05$) Pearson correlation coefficients for water quality measurements.

	Chl. <i>a</i>	Pheo.	Turb.	Total N	NO ₃ -N	NH ₄ -N	Total P	PO ₄ -P
Total chlorophyll, $\mu\text{g L}^{-1}$	0.999	0.971	-0.304	0.411	--	-0.314	-0.388	-0.548
Chlorophyll <i>a</i> , $\mu\text{g L}^{-1}$		0.966	-0.305	0.407	--	-0.316	-0.386	-0.544
Pheophytin, $\mu\text{g L}^{-1}$			-0.298	0.407	--	-0.303	-0.430	-0.596
Turbidity, NTU				0.336	--	0.598	0.732	0.624
Total N, mg L^{-1}					--	0.351	0.328	--
Dissolved NO ₃ -N, mg L^{-1}						--	-0.301	-0.335
Dissolved NH ₄ -N, mg L^{-1}							0.515	0.393
Total P, mg L^{-1}								0.909

Corellograms for some parameters, such as turbidity, were relatively flat throughout the range from 650 to 930 nm, while others had pronounced peaks and valleys. Particularly apparent were the maxima in the correlations to chlorophyll measurements at about 670 nm and the corresponding minima at about 705 nm. These features and the corresponding slope between them form the basis of two previously used approaches to optical chlorophyll estimation, the NIR/red ratio and the slope of the reflectance curve near 690 nm (e.g., Han and Rundquist, 1997).

Using the field spectrometer data, we applied these two approaches to estimate the three chlorophyll measurements, total chlorophyll, chlorophyll *a*, and pheophytin. Consistent with previous research, the slope (or derivative) approach provided better results than the ratio approach (table 4). Our estimations were somewhat less predictive than those ($r^2 = 0.38$ to 0.90) reported by Han and Rundquist (1997) for chlorophyll *a* estimation in a turbid reservoir in Nebraska. This difference in estimation accuracy may have been caused by the considerably higher chlorophyll levels and much lower turbidity levels in their data.

We also applied approaches from previous research to estimate turbidity levels. Han (1996) estimated turbidity based on the difference in reflectances between 710 and 720 nm, stating that this method was less susceptible to wind-induced waves on the water surface than data obtained at a single wavelength. Our model based on this approach yielded relatively poor results (equation 1; $r^2 = 0.44$).

$$\text{Turbidity (NTU)} = -10.83 + 2264 * (R_{710} - R_{720}) \quad (1)$$

In an outdoor tank study, Lodhi et al. (1998) found that spectrometer data, integrated into simulated Landsat-TM bands (LB), could be used to estimate suspended sediment concentration. We used this approach, assuming a linear relationship between sediment concentration and turbidity, to develop a first-order regression model for each simulated LB (table 5). In contrast to Lodhi et al. (1998), who found that a second-order model using simulated LB 4 (i.e., near infrared) reflectance was most predictive of sediment concentration, we found that a first-order model using the LB 4 data provided the best results. In this dataset, second-order parameters were not significant for any of the models, and models combining data from multiple bands were likewise not significant.

Table 4. Regression models for estimation of chlorophyll content using field spectrometer data.

Model	r ²	Std. Error
<u>NIR/red ratio models (NIR = reflectance at 705 nm; red = reflectance at 670 nm)</u>		
Total Chlorophyll (µg L ⁻¹) = -25.118 + 45.486 * (NIR/red)	0.42	17.0
Chlorophyll a (µg L ⁻¹) = -23.616 + 41.288 * (NIR/red)	0.42	15.2
Pheophytin (µg L ⁻¹) = -3.6123 + 10.751 * (NIR/red)	0.37	4.4
<u>Derivative models (slope = first derivative at 690 nm)</u>		
Total Chlorophyll (µg L ⁻¹) = 16.622 + 35204 * slope	0.60	14.0
Chlorophyll a (µg L ⁻¹) = 14.275 + 31940 * slope	0.61	12.5
Pheophytin (µg L ⁻¹) = 6.2820 + 8187.3 * slope	0.52	3.8

Table 5. Regression models for estimation of turbidity based on simulated Landsat-TM band (LB) reflectance calculated from field spectrometer data.

Model	r ²	Std. error
Turbidity (NTU) = -15.415 + 843.00 * LB1	0.56	14.5
Turbidity (NTU) = -15.544 + 531.08 * LB2	0.56	14.5
Turbidity (NTU) = -7.655 + 385.23 * LB3	0.62	13.5
Turbidity (NTU) = -0.734 + 801.90 * LB4	0.65	13.0

In addition to turbidity, simulated LB data were used to estimate other water quality parameters. Strong estimates were obtained only for total P and dissolved PO₄-P, with R² values of 0.93 and 0.89, respectively. In this data, these were the two measurements most strongly correlated with turbidity (table 3). The models obtained for estimating phosphorus concentrations using simulated LB data are given as equations 2 and 3.

$$\text{Total P (mg L}^{-1}\text{)} = 0.2014 - 10.711 \cdot \text{LB2} + 9.494 \cdot \text{LB3} \quad (2)$$

$$\text{Dissolved PO}_4\text{-P (mg L}^{-1}\text{)} = 0.1627 + 11.508 \cdot \text{LB1} - 18.470 \cdot \text{LB2} + 10.432 \cdot \text{LB3} - 3.794 \cdot \text{LB4} \quad (3)$$

Stepwise multiple linear regression, implemented in SAS Proc Stepwise (SAS Institute, Cary, N.C.), was also used to investigate the relationship of field spectrometer data to water quality parameters. Based on the scatter in figure 3, we deleted data above 930 nm, leaving 117 OD-transformed reflectance measurements as candidate independent variables. For each water quality parameter, the model with the most independent variables where all were significant ($\alpha = 0.05$) was selected. In a second analysis, we applied stepwise regression to the 26 field spectrometer bands most closely aligned with the bands present in the hyperspectral image data (table 1).

Using the full dataset, all water quality parameters were estimated with R² > 0.6 (table 6). Best estimates were obtained for the two phosphorus measurements, with R² > 0.9. Estimates of turbidity were least predictive, and were similar to those obtained using simulated LB data (table 5). Chlorophyll estimates using stepwise regression were considerably better than those obtained with previously reported approaches (table 4). Estimates of most parameters were of similar accuracy when using 26 candidate wavebands, suggesting the potential for good results with aerial hyperspectral image data.

Table 6. Statistics for best stepwise multiple linear regression models relating field spectrometer data to water quality parameters, both for the dataset containing all wavebands and for the 26 wavebands most closely corresponding to the aerial hyperspectral image data.

	117 candidate bands			26 candidate bands		
	R ²	Std. error	# of bands	R ²	Std. error	# of bands
Total chlorophyll, µg L ⁻¹	0.77	10.9	4	0.70	12.3	2
Chlorophyll a, µg L ⁻¹	0.82	8.99	6	0.70	11.1	2
Pheophytin, µg L ⁻¹	0.79	2.61	3	0.77	2.70	3
Turbidity, NTU	0.62	13.7	2	0.61	14.0	3
Total N, mg L ⁻¹	0.75	0.105	7	0.58	0.133	5
Dissolved NO ₃ -N, mg L ⁻¹	0.70	0.059	3	0.80	0.049	5
Dissolved NH ₄ -N, mg L ⁻¹	0.80	0.0084	7	0.76	0.0092	6
Total P, mg L ⁻¹	0.98	0.019	6	0.96	0.024	4
Dissolved PO ₄ -P, mg L ⁻¹	0.91	0.024	2	0.88	0.027	3

For all water quality parameters except turbidity, estimates obtained using stepwise regression on the full field spectrometer dataset, and on the 26-band subset, provided more accurate estimates than did previously developed spectral indices or regression on simulated LB multispectral data. For turbidity, results were slightly better using LB data, with approximately 7% lower standard error. These results indicate that hyperspectral data can provide better estimates of chlorophyll, nitrogen, and phosphorus concentrations in surface waters than can multispectral data, while multispectral data can successfully estimate turbidity or suspended sediment. Although these findings are consistent with past research, additional datasets, collected at differing lake levels and constituent concentrations, should be examined to ascertain the robustness of the estimation models.

Aerial Hyperspectral Image Data

The NIR/red ratio and derivative models were also applied to estimate chlorophyll content using aerial image data. Results using the ratio model were slightly worse for total chlorophyll and chlorophyll a than were results using the same model with field spectrometer data. Results using the derivative model were considerably less predictive for total chlorophyll and chlorophyll a but more predictive for pheophytin (table 7).

Stepwise regression applied to the 26-band (table 1) aerial hyperspectral data estimated all water quality parameters with R² > 0.6 (table 8). Some estimates were improved when the data used was an average of the 9 pixels centered on the measurement site, but this improvement was not consistent. Estimates with aerial data were generally of very similar accuracy to those obtained using the corresponding 26 bands of field spectrometer data (table 6), indicating that any additional errors introduced as part of the aerial image acquisition process did not greatly affect the use of the images for water quality estimation.

Table 7. Regression models for estimation of chlorophyll content using single-pixel aerial hyperspectral image data.

Model	r ²	Std. Error
<u>NIR/red ratio models (NIR = reflectance at 704 nm; red = reflectance at 673 nm)</u>		
Total Chlorophyll ($\mu\text{g L}^{-1}$) = $-175.27 + 201.45 * (\text{NIR/red})$	0.41	17.0
Chlorophyll a ($\mu\text{g L}^{-1}$) = $-155.90 + 178.81 * (\text{NIR/red})$	0.40	15.5
Pheophytin ($\mu\text{g L}^{-1}$) = $-46.521 + 55.100 * (\text{NIR/red})$	0.49	3.9
<u>Derivative models (slope = first derivative at 689 nm)</u>		
Total Chlorophyll ($\mu\text{g L}^{-1}$) = $13.319 + 137900 * \text{slope}$	0.47	16.2
Chlorophyll a ($\mu\text{g L}^{-1}$) = $11.517 + 122140 * \text{slope}$	0.45	14.8
Pheophytin ($\mu\text{g L}^{-1}$) = $5.0475 + 37901 * \text{slope}$	0.57	3.6

Table 8. Statistics for best stepwise multiple linear regression models relating aerial hyperspectral image data to water quality parameters, both for a single pixel at each site and for a 3- by 3-pixel average at each site.

	<u>single pixel</u>			<u>3- by 3-pixel average</u>		
	R ²	Std. error	# of bands	R ²	Std. error	# of bands
Total chlorophyll, $\mu\text{g L}^{-1}$	0.68	12.8	3	0.68	12.8	3
Chlorophyll a, $\mu\text{g L}^{-1}$	0.67	11.7	3	0.67	11.8	3
Pheophytin, $\mu\text{g L}^{-1}$	0.76	2.79	3	0.76	2.76	3
Turbidity, NTU	0.61	14.2	4	0.52	15.4	2
Total N, mg L^{-1}	0.70	0.113	6	0.62	0.125	4
Dissolved NO ₃ -N, mg L^{-1}	0.69	0.061	3	0.73	0.057	5
Dissolved NH ₄ -N, mg L^{-1}	0.57	0.0128	4	0.77	0.0090	4
Total P, mg L^{-1}	0.95	0.028	4	0.96	0.025	6
Dissolved PO ₄ -P, mg L^{-1}	0.98	0.013	7	0.97	0.015	5

As with the field spectrometer data, estimates of water quality parameters using aerial hyperspectral data were of promising accuracy. The fact that there was a wide range in the levels of these data among the different arms of the lake (table 2) gives some hope that the estimates may be robust to varying conditions encountered at different lake levels and/or times of the year. However, additional data collection under such varying conditions is needed to validate this approach to remote sensing of lake water quality.

Conclusions

Using hyperspectral data from either a field spectrometer or aerial images acquired on a single date, it was possible to estimate variations in water quality parameters (i.e., turbidity, chlorophyll, nutrients) in Mark Twain Lake in northeast Missouri. Best results ($R^2 > 0.6$ for all parameters) were obtained by applying stepwise regression to field spectrometer data from 117 candidate bands arrayed on a 5-nm spacing from 350 to 930 nm. Similar, but slightly less

predictive, results were obtained using data from 26 candidate bands, obtained either from a field spectrometer or an aerial image.

Using bands and approaches previously reported in the literature generally resulted in less predictive models than the stepwise modeling approach. However, these published approaches may be more robust to variations in ambient conditions and/or data collection procedures. Additional data collection is needed to verify the robustness of the results obtained in this study under a range of varying conditions.

Acknowledgements

The authors acknowledge the contributions of Harlan Palm and Brent Myers of the University of Missouri, and Scott Drummond, Lynn Stanley, and Joe Absheer of USDA-ARS to the collection, processing, and analysis of samples and data for this project.

References

- Han, L. 1996. Spectrometry of turbidity in surface water. In *Proc Int. Geoscience and Remote Sensing Symposium*, vol. 2, 1395-1397. Piscataway, N.J.: IEEE.
- Han, L., and D. C. Rundquist. 1997. Comparison of NIR/red ratio and first derivative of reflectance in estimating algal-chlorophyll concentration: a case study in a turbid reservoir. *Remote Sensing of Environment* 62: 253-261.
- Han, L., D. C. Rundquist, L. L. Liu, R. N. Fraser, and J. F. Schalles. 1994. The spectral responses of algal chlorophyll in water with varying levels of suspended sediment. *International Journal of Remote Sensing* 15(18): 3707-3718.
- Hayes, J. C., E. E. Godbold, and B. J. Barfield. 2001. Turbidity based on sediment characteristics for Southeastern U.S. soils. In *Proc. Int. Symp. on Soil Erosion Research for the 21st Century*, 408-411. J. C. Ascough II and D. C. Flanagan, eds. St. Joseph, Mich: ASAE.
- Lodhi, M. A., D. C. Rundquist, L. Han, and M. S. Kuzila. 1998. Estimation of suspended sediment concentration in water using integrated surface reflectance. *Geocarto International* 13(2): 11-15.
- Mausbach, M. J., and A. R. Dedrick. 2004. The length we go: Measuring environmental benefits of conservation practices. *Journal of Soil and Water Conservation* 59(5): 96A-103A.
- Nydahl, F. 1978. On the peroxodisulphate oxidation of total nitrogen in waters to nitrate. *Water Research* 12: 1123-1130.
- Ritchie, J. C., F. R. Schiebe, and J. R. McHenry. 1976. Remote sensing of suspended sediment in surface water. *Photogrammetric Engineering and Remote Sensing* 42: 1539-1545.
- Ritchie, J. C., P. V. Zimba, and J. H. Everitt. 2003. Remote sensing techniques to assess water quality. *Photogrammetric Engineering and Remote Sensing* 69(6): 695-704.
- Rundquist, D. C., L. Han, J. F. Schalles, and J. S. Peake. 1996. Remote measurement of algal chlorophyll in surface waters: the case for the first derivative of reflectance near 690 nm. *Photogrammetric Engineering and Remote Sensing* 62(2): 195-200.
- Shafique, N. A., F. Fulk, B. C. Autrey, and J. Flotemersch. 2003. Hyperspectral remote sensing of water quality parameters for large rivers in the Ohio River basin. In *Proc. First Interagency Conf. on Research in the Watersheds*, 216-221. K. G. Renard, S. A. McElroy, W. J. Gburek, H. E. Canfield, and R. L. Scott, eds. Washington, D.C.: USDA Agricultural Research Service.